Developmental Biology 398 (2015) 44–56

Contents lists available at ScienceDirect

Developmental Biology

journal homepage: www.elsevier.com/locate/developmentalbiology

PLR-1, a putative E3 ubiquitin ligase, controls cell polarity and axonal extensions in *C. elegans*

Jaffar M. Bhat, Jie Pan, Harald Hutter *

Department of Biological Sciences, Simon Fraser University, Burnaby, BC, Canada V5A 1S6

ARTICLE INFO

Article history:
Received 1 May 2014
Received in revised form
9 October 2014
Accepted 11 November 2014
Available online 20 November 2014

Keywords:
Neuronal development
Nervous system
Neuron
Pioneer
AVG
Axon guidance
Axon navigation
Cell polarity
E3 ligase
Wnt
C. elegans

ABSTRACT

During embryonic development neurons differentiate and extend axons and dendrites that have to reach their appropriate targets. In *Caenorhabditis elegans* the AVG neuron is the first neuron to extend an axon during the establishment of the ventral nerve cord, the major longitudinal axon tract in the animal. In genetic screens we isolated alleles of *plr-1*, which caused polarity reversals of the AVG neuron as well as outgrowth and navigation defects of the AVG axon. In addition *plr-1* mutants show outgrowth defects in several other classes of neurons as well as the posterior excretory canals. *plr-1* is predicted to encode a transmembrane E3 ubiquitin ligase and is widely expressed in the animal including the AVG neuron and the excretory cell. *plr-1* has recently been shown to negatively regulate Wnt signalling by removing Wnt receptors from the cell surface. We observed that mutations in a gene reducing Wnt signalling as well as mutations in *unc-53*/NAV2 and *unc-73*/Trio suppress the AVG polarity defects in *plr-1* mutants, but not the defects seen in other cells. This places *plr-1* in a Wnt regulation pathway, but also suggests that *plr-1* has Wnt independent functions and interacts with *unc-53* and *unc-73* to control cell polarity.

Introduction

The central nervous system consists of many neuronal circuits assembled in a precise manner. This is achieved by neuronal cell migrations and targeted outgrowth and navigation of individual neuronal processes (axons and dendrites). Navigation occurs through a complex environment during development by using conserved guidance cues and receptors (Goodman, 1996; Keynes and Cook, 1995; Tessier-Lavigne and Goodman, 1996) which is challenging due to the large number of neurons and potential navigational targets. The complexity of this navigation problem is reduced by the sequential outgrowth of axons. The first outgrowing axons are called 'pioneer' axons. These axons form a scaffold of axon tracts for later outgrowing 'follower' axons, which use these pre-established routes to extend along. Pioneer axons have been indentified in insects (Hidalgo and Brand, 1997; Klose and Bentley, 1989) and vertebrates (Chitnis and Kuwada, 1991; McConnell et al., 1989). In *Caenorhabditis elegans*, a single neuron, AVG, located at the anterior end of the ventral nerve cord (VNC) is the first neuron to send out an axon towards the posterior end of the body along the right side of the ventral nerve cord (Durbin, 1987). AVG is required for correct navigation of follower axons, because its removal leads to a disorganized ventral nerve cord with misguided axons (Durbin, 1987; Hutter, 2003).

C. elegans has a simple nervous system with axon tracts mainly running in parallel to the anterior–posterior (AP) and the dorso-ventral (DV) axis. Several guidance cues including UNC-6/netrin (Hedgecock et al., 1990; Ishii et al., 1992), SLT-1 (Hao et al., 2001) and the TGF-β/UNC-129 (Colavita et al., 1998) are known to guide the migration of cells and axons along the dorso-ventral axis. In contrast, few key players in the anterior–posterior migrations have been identified. UNC-53/NAV2 a cytoskeletal regulator has defects in both anterior and posterior axonal extensions and also shows guidance defects in many cell types (Stringham et al., 2002). VAB-8 is a cytoplasmic protein with kinesin-like motor domain and is required specifically for posterior-directed migrations (Wightman et al., 1996; Wolf et al., 1998). Wnts are known to control anterior–posterior polarity of neurons as well as certain cell migrations along the anterior–posterior axis (Hilliard and Bargmann, 2006; Pan et al., 2006). In contrast to many of the genes implicated in dorso-ventral guidance, which act globally, the known genes acting in anterior–posterior migrations have a more limited role affecting only some migrations.

The guidance cues used by the ventral nerve cord pioneer AVG are largely unknown (Hutter, 2003). Here we describe the roles of *plr-1* in axonal outgrowth and establishment of cell polarity. We

* Corresponding author. Fax: +1 778 782 3496.
E-mail address: hutter@sfu.ca (H. Hutter).

http://dx.doi.org/10.1016/j.ydbio.2014.11.008
0012-1606/

isolated two alleles of *plr-1*, *hd128* and *hd129*, in genetic screens for AVG axon guidance defects. *plr-1* mutants show various defects in the outgrowth and navigation of the AVG axon including premature stop, navigation defects in the VNC and polarity reversal leading to an extension of the primary neurite in anterior rather than posterior direction. In addition *plr-1* mutants show defects in posterior extension of the AVK and CAN axons as well as posterior excretory canals, and migration and axonal navigation defects in HSN neurons. *plr-1* is predicted to encode an E3 ligase containing a transmembrane domain and a RING finger domain and is expressed in a variety of tissues including some cells affected in *plr-1* mutants. PLR-1 has recently been shown to remove Wnt receptors from the surface of the AVG neuron controlling polarity of the neuron (Moffat et al., 2014). Here we show that *plr-1* also interacts genetically with *unc-53*/NAV2 and *unc-73*/Trio in the context of regulating AVG polarity. In addition we demonstrate that reduced Wnt signalling restores AVG polarity, but does not rescue other defects seen in *plr-1* mutants, suggesting that *plr-1* has Wnt-independent functions as well.

Results

plr-1 mutant animals show polarity reversal and axon outgrowth defects in the ventral nerve cord pioneer AVG

Two alleles of *plr-1*, *hd128* and *hd129*, were isolated in genetic screens for AVG axon outgrowth defects. A third allele, *tm2957*, was kindly provided by the Mitani lab. The genetic screens were performed with a marker strain (*odr-2*::*tdTomato*) that allowed us to visualize the left and right VNC axon tracts in addition to the AVG axon in the right tract. This enabled us to detect navigation errors where the AVG axon crosses the ventral midline to extend in left axon tract referred to as crossover defects. All three *plr-1* alleles showed crossover defects with a similar penetrance of 15–18% (Fig. 1G, Table 1). In a small number of animals, 3% in *plr-1* (*hd129*), the AVG axons left the ventral cord (Fig. 1H, Table 1). The most prominent AVG defect, found in more than half of the *plr-1* (*hd129*) mutant animals, is a premature stop of the AVG axon at various positions along the ventral cord (Fig. 1C and D, Table 1). The penetrance of this defect ranged from 52% in *plr-1*(*hd129*) to 17% in *plr-1*(*hd128*). Overall *hd129* mutant animals displayed the most penetrant defects, *tm2957* mutants were less severely affected and *hd128* mutants showed the weakest defects (Table 1).

The AVG neuron normally extends a very short process anteriorly and a long process posteriorly (Fig. 1A and B). The marker strain used for the initial analysis labels additional neurons in the head, preventing any analysis of AVG's anterior process. Analysis of the AVG defects with a marker strain that selectively labels AVG (*inx-18*::GFP) revealed that in a substantial fraction of *plr-1* mutant animals the AVG neuron had a long anterior and very short posterior process (Fig. 1E and F, Table 1). Similar defects have been found by Moffat et al. (2014) and have been shown to be the result of a reversal of the anterior–posterior polarity of AVG. In addition there are many animals, where the polarity of AVG is normal (defined as AVG having a very short anterior process and a long posterior process), but the AVG axon stops prematurely in the VNC (Fig. 1C and D, Table 1).

plr-1 mutant animals show cell migration, axon extension and axon guidance defects in a variety of neurons

Previous phenotypic analysis of *plr-1* mutants was limited to defects seen in AVG (Moffat et al., 2014). To determine whether *plr-1* mutants have defects in other neurons, we examined additional neurons using cell type-specific markers in the strongest allele, *hd129*. We found that *plr-1*(*hd129*) mutant animals had cell migration and axon navigation defects in HSN neurons (Fig. 2A and B, Table 2). In 26% of *plr-1*(*hd129*) mutant animals, the HSN cell bodies were found at variable positions posterior to their normal location around the vulva (Table 2). In 48% of the animals, where the HSN cell bodies were correctly positioned and the HSN axons extended into the VNC, we found that HSN axons inappropriately crossed the ventral midline to extend in the contralateral axon tract (Fig. 2A and B, Table 2).

Under normal conditions axons of the AVK neurons extend in the VNC all the way to the posterior end of the cord (Fig. 2C). However, in *plr-1*(*hd129*) animals we observed AVK axons frequently failing to reach their normal termination point (Fig. 2D). In most cases both AVK axons stop prematurely and in all cases the axons extend past the vulva, i.e. more than halfway towards the target (Table 2), suggesting that none of these defects are due to a reversal in the polarity of the neurons. CAN neurons have one anterior and one posterior processes of comparable length, extending from the cell body in a lateral position (Fig. 2E). In *plr-1*(*hd129*) animals the posterior process often terminates short of its normal destination (Fig. 2F, Table 2). As with AVK, the process always extends at least halfway to its target. In addition a fraction of animals display branching and/or navigation defects (Table 2). The anterior CAN process was unaffected in *plr-1* mutant animals.

Since processes from CAN neurons extend in close proximity to the excretory canals and studies suggested CAN neurons have a role in regulating the adjacent excretory canals (Hedgecock et al., 1987), we wanted to test whether excretory canals were also affected. The cell body of the excretory cell lies on the ventral side in the head region of the animal. The cell extends two shorter anterior and two longer posterior canals extending in lateral position all the way to the tail (Fig. 2G). We found that some *plr-1*(*hd129*) animals had excretory canals that terminated short of the normal position (Fig. 2H, Table 2). Again the terminating points were all in the posterior half of the animal, indicating that the canals extend most of the distance. Anterior canals were not affected. Excretory canal defects are much less penetrant than CAN defects, suggesting that these defects in *plr-1* mutants are independent.

Using additional markers we found no significant defects in the migration of the Q neuroblasts, nor in the migration and axonal navigation of the touch receptor neurons, the GABAergic DD/VD and cholinergic DA/DB motor neuron axons, the PVP/PVQ axons in the VNC or the ASH dendrite and axon in the head (Table 3). We did observe mild navigation and premature stop defects in *glr-1*::GFP expressing interneurons, which normally extend in the right VNC tract (Table 3). Since navigation of these axons in part depends on the pioneer AVG, it is possible that these interneuron defects are secondary consequences of AVG defects. We found no polarity defects in neurons with cell bodies close to AVG (RIF and RIG neurons) or in other neurons, whose polarity is affected by Wnt signalling (touch neurons), suggesting that the polarity defects in *plr-1* mutants are specific to AVG (Table 3).

In summary, *plr-1* mutant animals are characterized by a polarity reversal defect of the AVG neuron and show a number of axonal extension and navigation defects in a small number of unrelated neurons located throughout the animal.

plr-1 encodes a monomeric RING finger protein

We mapped *plr-1*(*hd129*) to a 337.6 kb interval on chromosome III using snip-SNP markers. Rescue experiments with genomic fosmid clones identified a single fosmid containing two genes (Fig. 3A). Rescue experiments with individual genes revealed that *plr-1*/*Y47D3B.11* was the only gene able to rescue the AVG defects in *plr-1* mutants. Sequencing of *hd128* and *hd129* alleles identified

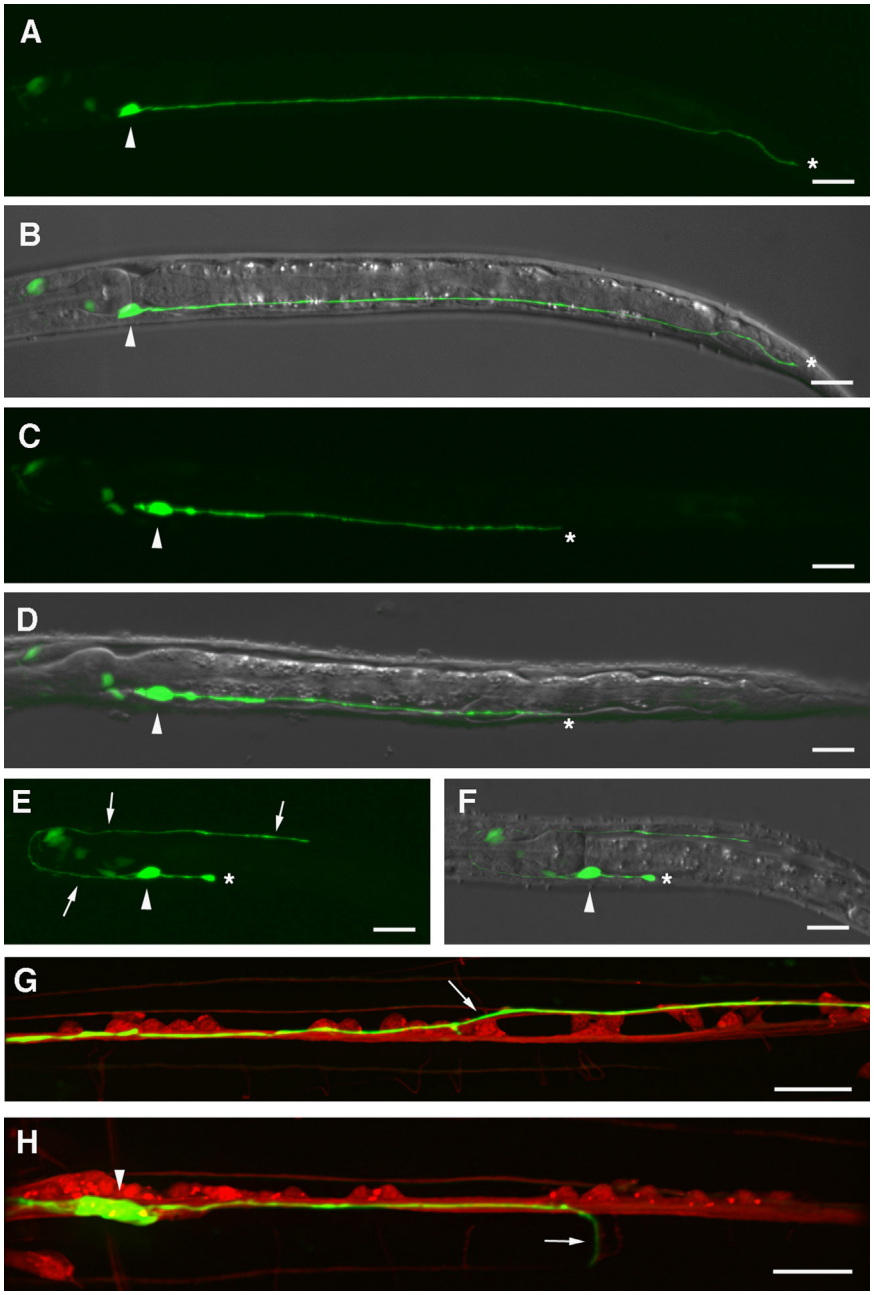

Fig. 1. AVG defects in *plr-1*(*hd129*) mutant animals. (A, B) Wild type L1, side view; the AVG cell body (arrowhead) is located at the anterior end of the ventral nerve cord. The axon extends along the entire length of the animal on the ventral side and terminates in the tail region (asterisk). (C, D) In *plr-1*(*hd129*) mutant animals the AVG cell body is in its normal position (arrowhead), but the axon stops prematurely (asterisk). (E, F) In *plr-1*(*hd129*) mutant animals AVG sends out a short posterior process (asterisk) and a long anterior process that grows into the head (arrows), indicating a reversal of cell polarity. (G) In *plr-1*(*hd129*) mutant animals the AVG axon crosses the midline and joins the left ventral cord axon tract (arrow). (H) In some mutant animals the AVG axon leaves the ventral nerve cord (arrow). (A, C, E) GFP channel. (B, D, F) Overlay of Nomarski and GFP channel. (G, H) Overlay of GFP and DsRed channels. Scale bar: 20 μm. Markers used: *otIs182* (*inx-18*::GFP) for AVG (green) and *evIs111* (*rgef-1*::*DsRed*) as panneuronal marker in panel G, H.

mutations in *Y47D3B.11* (Fig. 3B), confirming the identity of *plr-1*. The independently isolated *tm2957* allele showed similar AVG defects, further supporting the idea that *plr-1* is *Y47D3B.11*.

plr-1 encodes a protein with a predicted size of 487 amino acids. Its predicted domains include a signal peptide, a transmembrane domain, and a single RING finger domain (Fig. 3C). It is classified as one of the 152 monomeric RING finger proteins in *C. elegans*. The presence of a signal peptide and transmembrane domain suggests that the protein enters the secretory pathway and is either located at the cell surface or in membrane-bound intracellular compartments that originate from the endoplasmic reticulum. Putative homologues of PLR-1 in mammals are RNF43 and ZNRF3 (Hao et al., 2012; Koo et al., 2012). All three proteins are similar in the N-terminal part up to and including the RING finger domain, but are divergent in the C-terminus with both RNF43 (784 amino acids) and ZNRF3 (913 amino acids) being substantially larger than PLR-1.

All three *plr-1* alleles are small deletions in the gene. *hd129* is a 159 bp deletion missing exon 2 and some flanking intronic sequences (Fig. 3B). This deletion is expected to produce a frameshift and a stop codon truncating the protein after 79 amino acids (Fig. 3C). *hd128* is a 132 bp in-frame deletion in exon 4, just C-terminal of the transmembrane domain (Fig. 3B and C). *tm2957* is a 239 bp deletion at the beginning of exon 4 resulting in a frameshift and truncation after 154

amino acids (Fig. 3B and C). Based on the molecular nature of the alleles, *hd129* is expected to be the strongest loss-of-function allele, likely a null allele. *hd128* is expected to be the weakest allele. Consistent with our expectations, *hd129* showed the strongest defects, and *hd128* showed the weakest defects.

plr-1 is widely expressed throughout development

To identify cells expressing *plr-1* we generated transgenic animals expressing green fluorescent protein (GFP) under the control of a 3.9 kb promoter fragment. *plr-1*::GFP expression became visible in late gastrulation stage embryos (Fig. 4A and B). Strongest expression was detected in many cells in the tail region and by comma stage the most prominent expression was seen in body wall muscle cells (Fig. 4C and D). In early larval stages expression was detectable in a number of different tissues including the major hypodermal cells, muscle and marginal cells of the pharynx, the intestine (strongest in the anteriormost and posteriormost cells) as well as the anal depressor and stomatointestinal muscle (Fig. 4E and F). In the nervous system GFP expression was visible in a few neurons in head ganglia, many ventral cord motor neurons and several neurons in the tail ganglia including the PDA neuron (Fig. 4E and F). Based on the lack of commissures the motor neurons are likely of the VA, VB, VC and/or AS class. Based on the number of cells the majority (or even all) of these classes express GFP. In general expression was strongest in the tail region throughout development. This also held true for the motor neurons in the ventral cord, where GFP was strongest in the posterior-most cells and barely detectable in anterior motor neurons. Expression is maintained throughout larval development. In later larval stages expression is also seen occasionally in the distal tip cell of the developing gonad, the vulva and uterine muscle cells and the VC4 and VC5 neurons flanking the vulva (Fig. 4G and H). Expression in AVG, HSN or CAN neurons was not detectable with this reporter construct, but was detected in a previous study in HSN and CAN using a longer genomic construct (Moffat et al., 2014).

To determine the subcellular localization of PLR-1 we fused GFP to the C-terminus of the *plr-1* coding sequence in a fosmid containing the entire *plr-1* gene and surrounding genomic DNA. This construct was able to rescue the AVG defects, indicating that it is functional. PLR-1::GFP expression levels are variable, but generally fairly low.

Table 1
AVG defects in *plr-1* mutants (% animals with defects).

Phenotype	Wild type	*plr-1* (*hd129*)	*plr-1* (*tm2957*)	*plr-1* (*hd128*)
Marker: odr-2::*tdTomato*	*n*=117	*n*=139	*n*=69	*n*=135
Premature stop[a]	0	52**	38**	17**
VNC cross-over[b]	0	18**	17**	15**
Leaving VNC	0	3[ns]	3[ns]	0
No defect	100	27**	42**	68**
Marker inx-18::*gfp*	*n*=150	*n*=166	*n*=121	*n*=108
Polarity reversal	0	46**	34**	7**
Premature stop[c]	0	33**	21**	31**
Leaving VNC	0	2[ns]	2[ns]	1[ns]
No defect	100	19**	43**	61**

All mutant phenotypes are significantly different from wild type ($p < 0.01$) except leaving VNC phenotype.

[a] Will include animals with polarity reversal.
[b] Some animals have cross-over and premature stop defects.
[c] Does not include animals with reversed polarity.
** $p < 0.01$.
[ns] Not significant; χ^2 test.

Table 2
Other neuronal defects in *plr-1*(*hd129*) mutant (% animals with defects).

Phenotype	Wild type	*plr-1*(*hd129*)
HSN defects		
HSN migration defects[a]	5 (107)	26** (97)
HSN VNC cross-over defects[b]	16 (107)	48** (97)
CAN defects (*posterior axons*)		
Premature stop[c]	0 (150)	82** (116)
Navigation defect[d]	0 (150)	12** (116)
Branching defect[e]	0 (150)	6** (116)
Other defects		
Premature stop of AVK axons[f]	0 (160)	87** (108)
Premature stop of posterior excretory canals[g]	5 (104)	39** (103)

Value in brackets indicates *n*.
Markers used: HSN (*tph-1*::*GFP*), CAN (*ceh-23*::*GFP*), AVK (*flp-1*::*GFP*) and excretory canal (*pgp-12*::*GFP*).

[a] At least one HSN neuron is located posterior to the vulva.
[b] Only scored in animals without HSN migration defects.
[c] Both posterior axons stop prematurely at variable positions.
[d] One axon makes a U-turn and grows anteriorly before stopping.
[e] One axon branches shortly before stopping prematurely.
[f] Both AVK axons stop prematurely at variable positions posterior to the vulva.
[g] One or both excretory canals stop prematurely at variable positions posterior to the vulva.
** $p < 0.01$; χ^2 test.

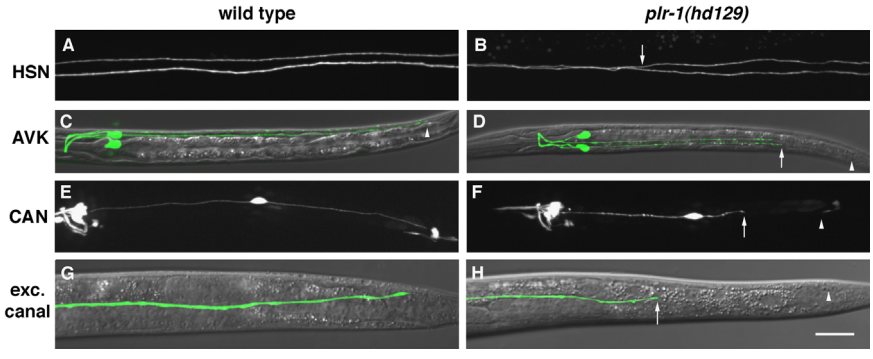

Fig. 2. Other neuronal and non-neuronal defects in *plr-1*(*hd129*) mutant animals. (A, C, E, G) wild type; (B, D, F, H) *plr-1*(*hd129*). (A) In wild type animals HSN axons grow in both ventral nerve cord axon tracts and never cross the midline. (B) In *plr-1*(*hd129*) mutant animals HSN axons cross the midline (arrow). (C) In wild type animals AVK axons extend in both ventral nerve cord axon tracts and terminate in the tail (arrowhead). (D) In *plr-1*(*hd129*) mutant animals AVK axons terminate prematurely in the posterior half of the animal (arrow, the arrowhead indicates the normal stopping point). (E) In wild type animals CAN neuron sends out two processes in opposite directions. The posterior process terminates in the tail region. (F) In *plr-1*(*hd129*) mutant animals the posterior CAN process terminates prematurely in the posterior half of the animal (arrow, normal termination point is indicated by arrowhead). (G) In wild type animals the posterior excretory canal terminates in the tail region. (H) In *plr-1*(*hd129*) mutant animals the posterior excretory canal terminates prematurely (arrow, arrowhead indicates normal termination point). Markers used: AVG marker (*odr-2*::*tdTomato*), AVK marker (*flp-1*::GFP), CAN marker (*ceh-23*:: GFP), HSN marker (*tph-1*:: GFP) and excretory canal marker (*pgp-12*:: GFP). Scale bar: 20 μm.

Table 3
Low penetrant neuronal defects in *plr-1*(*hd129*) mutant (% animals with defects).

Phenotype	Wild type	*plr-1*(*hd129*)
Interneuron defects		
Premature stop	0 (101)	11** (131)
Navigation defect	0 (101)	5* (131)
Touch receptor neuron defects		
Ventral synapses missing	0 (110)	4* (92)
PLM premature stop	0 (110)	2^{ns} (92)
PVP and PVQ defects		
Navigation defects	7 (118)	8^{ns} (109)
Overextension	0 (118)	13** (109)
ASH neuron defects	0 (103)	0 (110)
RIF neuron defects	0 (103)	0 (111)
Motor neuron defects		
DD/VD	0 (110)	0 (72)
DA/DB	0 (85)	0 (105)
Commissures	0 (90)	0 (87)
Q neuroblast migration defects	0 (112)	0 (142)

Values in brackets indicate *n*.
Markers used: interneuron (*glr-1*::*GFP*), touch receptor (*mec-4*::*GFP*), PVP/PVQ/ ASH (*odr-2*::*CFP*, *sra-6*::*DsRed*), RIF (*odr-2*::*DsRed*), DD/VD/commissures (*unc-47*::*DsRed2*), DA/DB (*unc-129*::*CFP*) and Q neuroblast migration (*rgef-1*::*GFP*).
* $p < 0.05$.
** $p < 0.01$.
^{ns} Not significant; χ^2 test.

The GFP signal is concentrated in puncta spread throughout the cytoplasm mainly in the cell body, but also extends into neuronal processes. GFP expression is detectable in comma stage embryos (Fig. 5A and B) with strongest expression in the tail region. The distinct subcellular localization makes it difficult to confirm cell identities, but overall expression is comparable to the *plr-1*::GFP promoter construct. Postembryonical GFP expression in the head region seems restricted to some neurons and the posterior region of the pharynx. Expression was not readily detectable in hypodermal or body wall muscle cells with this construct postembryonically. Expression of the PLR-1::GFP fusion protein, however, is detectable in the AVG neuron and also in the excretory cell (Fig. 5D–G). This suggests that the promoter construct lacks some control elements. Since the GFP expression of the fusion protein is significantly lower than the expression of the promoter construct, it is possible that low levels of expression in tissues and cells expressing the *plr-1*::GFP transcriptional reporter remain undetectable. The punctate expression of PLR-1::GFP fusion protein (Fig. 5G) suggests that PLR-1 is present in some endocytotic compartments. Recently PLR-1 has been shown to colocalize with endosomal markers (Moffat et al., 2014), suggesting that PLR-1 indeed enters the secretory pathway.

mig-14/Wntless mutants partially suppress the plr-1 defects

PLR-1 and its vertebrate homologues RNF43 and ZNRF3 have been shown to downregulate Wnt receptors (Hao et al., 2012; Koo et al., 2012; Moffat et al., 2014). In *C. elegans* AVG polarity reversal defects have been linked to excessive Wnt signalling, since mutations in the Wnts *cwn-1* and *cwn-2* suppress the polarity defects in AVG (Moffat et al., 2014). Furthermore *plr-1* has been shown to reduce cell surface levels of Wnt receptors in AVG and ectopic expression of *plr-1* can block Wnt signalling (Moffat et al., 2014). We wanted to determine whether all defects seen in *plr-1* mutants can be suppressed by reducing Wnt signalling. *C. elegans* has five Wnt genes with overlapping functions (Pan et al., 2006; Yamamoto et al., 2011). Secretion of all Wnts requires the activity of the Wntless (*mig-14* in *C. elegans*) gene (Banziger et al., 2006; Yang et al., 2008). While a complete loss of function of *mig-14* is lethal due to the importance of Wnt signalling in early embryonic development, viable partial loss-of-function alleles exist (e.g. *ga62*). Those alleles are considered to have a reduced level of Wnt signalling (Eisenmann and Kim, 2000; Harris et al., 1996; Yang et al., 2008). We generated *mig-14*(*ga62*); *plr-1*(*hd129*) double mutants and evaluated the various defects seen in *plr-1* single mutants. We found that *mig-14*(*ga62*) was able to strongly suppress the polarity reversal, axonal stop and axonal navigation defects of AVG (Fig. 6), confirming that these defects are due to ectopic Wnt signalling as previously observed (Moffat et al., 2014). In contrast, the premature termination defects of the AVK and CAN axons as well as the premature stop of the excretory canals were not effectively rescued (Fig. 6). *mig-14*(*ga62*) mutants themselves have HSN migration defects, which makes it impossible to evaluate a potential rescue of the HSN defects in *plr-1*. Both *plr-1* animals and *mig-14*; *plr-1* animals show similar penetrant excretory canal defects, suggesting that the two genes act in the same genetic pathway here (Fig. 6). These data suggest that *plr-1* has both Wnt-dependent and Wnt-independent roles.

unc-53 and unc-73 mutants suppress AVG polarity reversal defect of plr-1 mutants

UNC-53/NAV2 is a cytoskeleton regulator (Stringham and Schmidt, 2009) important for longitudinal migrations in *C. elegans* (Stringham et al., 2002). In *C. elegans*, *unc-53* mutant animals did not display AVG axon defects (Fig. 7A), but have short posterior excretory canals similar to *plr-1* mutants. While testing genetic interactions of *plr-1* and *unc-53* in excretory canal extensions (see below) we found unexpectedly that the polarity reversal defects of AVG axon are completely suppressed in *unc-53*; *plr-1* animals (Fig. 7A). We also observed that the majority of AVG axons in *unc-53*; *plr-1* animals terminate prematurely (Fig. 7B), which suggests that *unc-53* also plays a role in the posterior extension of AVG axon. *unc-53* does not suppress the AVK, CAN, HSN and excretory canal defects found in *plr-1* mutants (Fig. 7C), suggesting that interactions between *unc-53* and *plr-1* are limited to phenotypes related to AVG.

Mutations in *unc-73*/*Trio* encoding a Rac/Rho guanine nucleotide exchange factor (GEF) lead to a variety of axonal navigation defects including some premature stop defects of the AVG axon (Fig. 7B). UNC-73/Trio has separate GEF domains for Rho and Rac and has different isoforms: UNC-73B interacts with Rac and UNC-73E interacts with Rho. We obtained isoform specific mutants affecting either of these domains and constructed double mutants with *plr-1*. We found a partial suppression of the *plr-1* AVG polarity reversal defects in *unc-73B*(*rh40*); *plr-1* and *unc-73E*(*ev802*); *plr-1* double mutants (Fig. 7A). In both *unc-73*; *plr-1* double mutants the premature termination defect of the AVG axon was enhanced compared to *plr-1* single mutants (Fig. 7B), suggesting that *unc-73* is acting independently of *plr-1* in the posterior extension of AVG axon.

VAB-8 is a cytosolic protein with a kinesin-like motor domain at the N-terminus promoting posterior cell migrations and axon guidance together with UNC-73 and UNC-53 (Marcus-Gueret et al., 2012; Wightman et al., 1996; Wolf et al., 1998). *vab-8* single mutants show some premature termination of the AVG axon (data not shown) but do not display AVG polarity reversal defects. In *vab-8*; *plr-1* double mutants the AVG polarity reversal defects of *plr-1* are enhanced to 100% (Fig. 7A) in striking contrast with the observations in *unc-53*; *plr-1* and *unc-73*; *plr-1* double mutants, suggesting that *vab-8* does not act in the same pathway as *unc-53* and *unc-73* in this context.

plr-1 acts through a novel pathway to control posterior extension of excretory canals

The posterior extension of excretory canals is controlled by two distinct parallel pathways (Marcus-Gueret et al., 2012). In

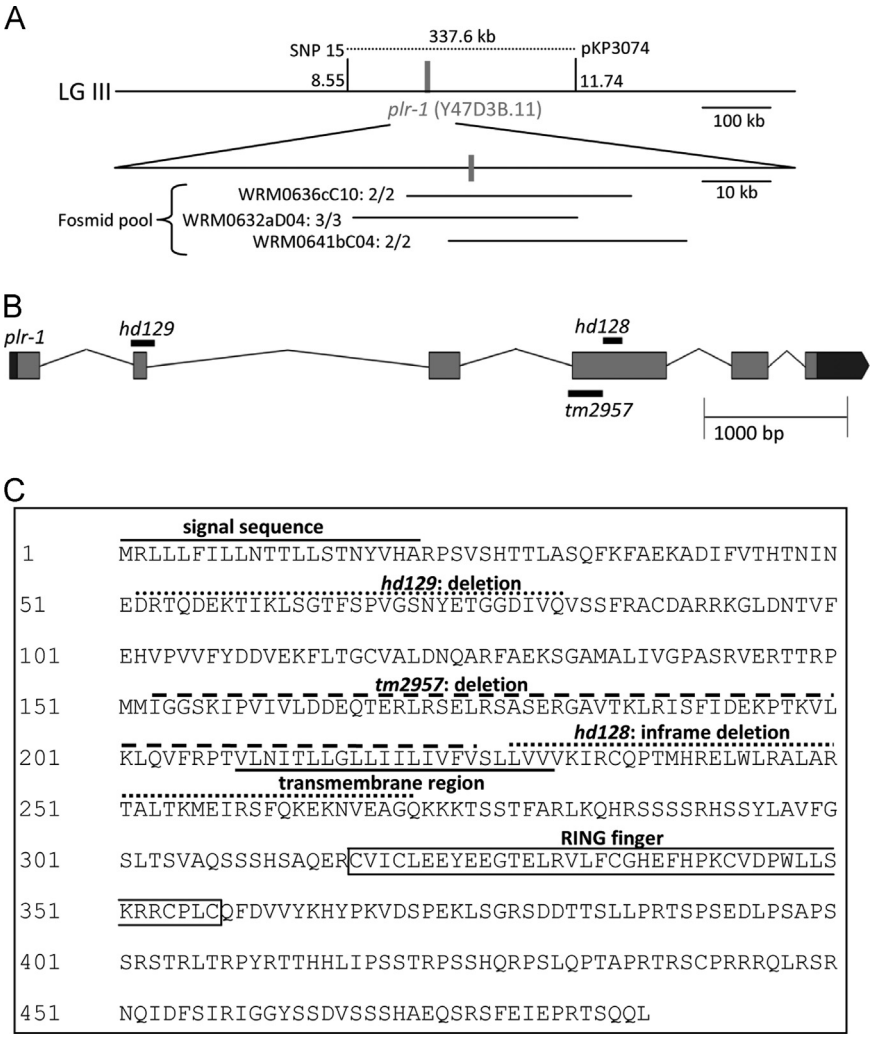

Fig. 3. Molecular analysis of *plr-1*. (A) Schematic drawing of the genomic region on the chromosome III (LG III) containing the *plr-1* gene. Numbers next to fosmid names (e.g. WRM0636cC10) indicate the fraction of transgenic lines rescuing the *plr-1* defects (e.g. 2/2). 'Fosmid pool' refers to a mixture of all the fosmids used for the initial rescue. The only gene contained in all fosmids is Y47D3B.11 (B) Gene model for *plr-1* with exons shown by light grey shaded boxes. The black shaded boxes in the beginning and end represent the 5′ and 3′ UTRs respectively. The location of alleles used in this study is indicated by black bars. *hd129* is a 159 bp deletion removing whole exon 2 and adjoining parts of intron 1 and intron 2, which changes the reading frame and leads to the formation of stop codon. *tm2957* is a 239 bp deletion in the beginning of axon 4 which also changes the reading frame and leads to the formation of a stop codon. *hd128* is a 132 bp inframe deletion within axon 4. (C) PLR-1 amino acid sequence highlighting the signal sequence (SS), transmembrane (TM) and RING domains based on SMART analysis (http://smart.embl-heidelberg.de). Changes induced by *plr-1* mutations are also indicated. The *hd129* and *tm2957* deletions create frameshits and would lead to premature stop codons leading to truncated proteins of 79 aa and 154 aa respectively.

one pathway, VAB-8 interacts with the receptor SAX-3 and the RacGEF form of UNC-73 outside the excretory cell. In addition UNC-53 interacts with the RhoGEF form of UNC-73 and many components of cytoskeleton in the excretory cell itself. We wanted to test if *plr-1* acts in any of these two pathways. Given the expression of *plr-1* in excretory cell, one would expect *plr-1* to act in a cell autonomous manner possibly together with *unc-53*. To test this hypothesis, we chose components from both of these pathways for double mutant analysis with *plr-1*. In both *unc-53*; *plr-1* and *vab-8*; *plr-1* double mutants the excretory canal defects are stronger compared to the strongest single mutant (Fig. 8). These data suggest that *plr-1* does not act in these pathways. We further tested the RacGEF and RhoGEF forms of UNC-73/Trio. In both *unc-73E*(*ev802*); *plr-1* and *unc-73B*(*rh40*); *plr-1* double mutants the defects are stronger compared to the strongest single mutants (Fig. 8), confirming the idea that *plr-1* acts through a novel parallel pathway to control the posterior extension of excretory canals. Given these observations we expressed PLR-1 specifically in excretory cell to determine whether PLR-1 is required in the excretory cell for proper excretory canal extensions. We examined the excretory canal defects in transgenic lines expressing a PLR-1 cDNA construct tagged with GFP specifically in excretory cell. We found that PLR-1 was able to rescue the excretory canal defects in three out of three independent transgenic lines ($n > 100$). This strongly suggests that PLR-1 is required in the excretory cell for excretory canal extension and acts in a cell autonomous manner.

plr-1 interacts with the unc-73/Trio for the correct navigation of AVG axon

In *plr-1* mutant animals the AVG axon crosses the midline and joins the contralateral tract in a significant fraction of animals (30%), suggesting a navigation defect likely due to a failure to respond to guidance cues. *sax-3*/*Robo*, *unc-6*/*Netrin* and *nid-1*/*Nidogen* mutants show similar midline crossing defects albeit with a lower penetrance (Hutter, 2003). To determine if *plr-1* genetically interacts with these genes for AVG axon navigation, double mutants were made with *plr-1*. In all cases we observed that the penetrance of AVG navigation defects in double mutants was not

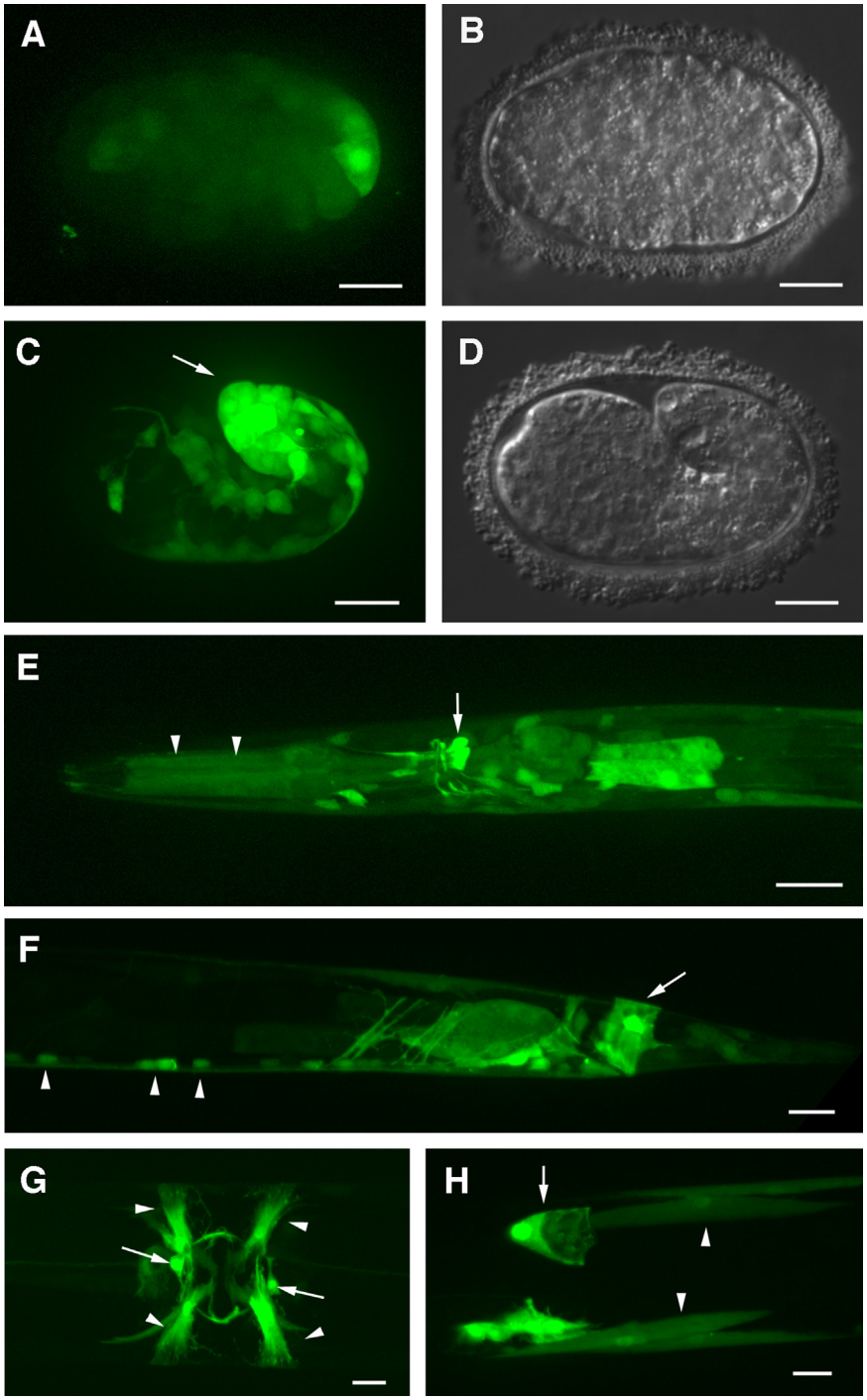

Fig. 4. Expression pattern of a *plr-1*::GFP transcriptional reporter construct. (A, B) Late gastrulation stage embryo. GFP is expressed in a large number of cells throughout the embryo. Posterior cells express GFP more strongly. (C, D) 1½ fold stage embryo. Expression is strongest in the tail region in hypodermal and muscle cells (arrow). (E) In larvae expression is seen in a few neurons in the head (arrow), the marginal cells in the pharynx (arrowheads) as well as hypodermal cells. (F) In the tail region of larvae expression is seen in motor neurons in the ventral nerve cord (arrowheads) and the anal depressor muscle (arrow). (G) In the vulva region expression is seen in the VC4 and VC5 neurons (arrows) and the vulva muscle cells (arrowheads). (H) Expression is also seen in the distal tip cells of the developing gonad (arrow) and body wall muscle cells (arrowheads). (B, D) Nomarksi images, the other panels are fluorescent confocal images. Scale bars: 10 μm (A–D), 20 μm (E–H).

significantly different from *plr-1* single mutants (Fig. 9), but also not significantly different from the sum of the two individual mutants. This suggests that *plr-1* does not act synergistically with any of these genes.

UNC-73/Trio mediates axonal responses to several guidance cues including Netrin and Slit (Watari-Goshima et al., 2007). We observed that *unc-73B*(*rh40*) which affects the RacGEF domain of UNC-73/Trio has midline crossing and premature termination defects of the AVG axon (Fig. 9). AVG midline crossing defects are suppressed in *plr-1*; *unc-73B*(*rh40*) double mutants as compared to *plr-1* single mutants (Fig. 9). *unc-73E*(*ev802*) mutants affecting the RhoGEF domain of UNC-73/Trio show only few midline crossing and no premature termination defects of the AVG axon. *plr-1*; *unc-73E*(*ev802*) double mutant is similar to *plr-1* single mutant (Fig. 9), suggesting the interactions between *unc-73* and *plr-1* are limited to the RacGEF isoform of *unc-73*.

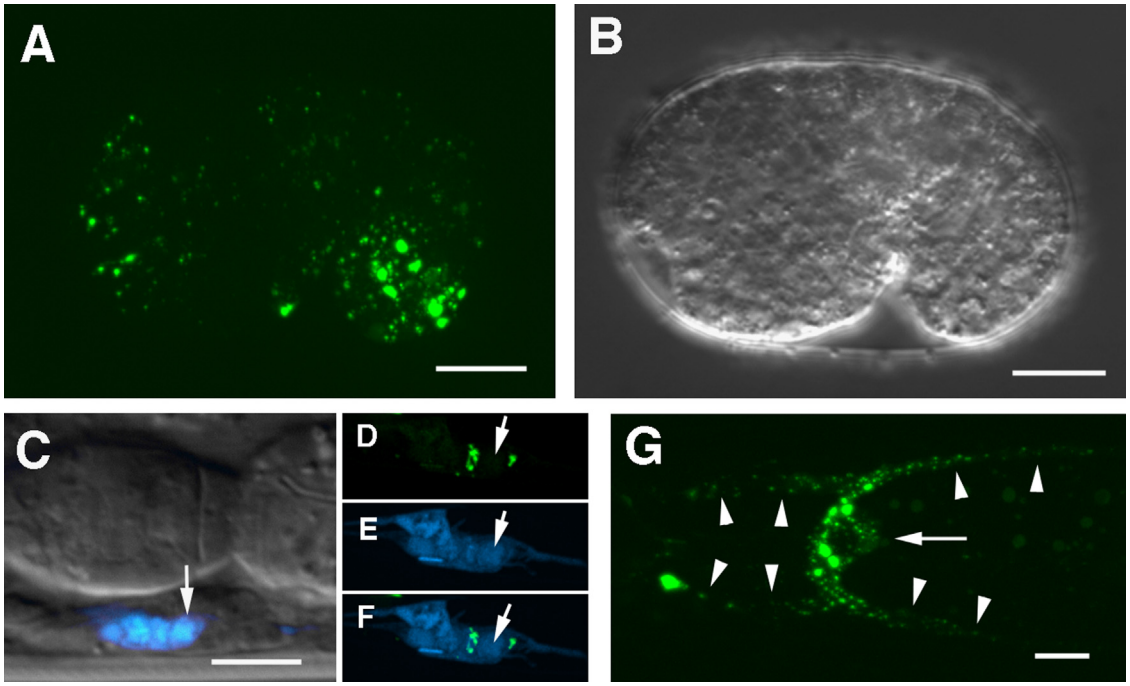

Fig. 5. Expression pattern of a functional PLR-1::GFP protein fusion construct. (A, B) Comma stage embryo. Expression is seen throughout the embryo with the strongest expression in the tail region. The PLR-1::GFP fusion protein is localized to variable-sized puncta throughout the cytoplasm. (C–F) In larval stages expression can be detected in the AVG neuron (arrowhead). (G) Expression is also seen in the excretory cell, where PLR-1::GFP puncta are concentrated in the cell body (arrow) and in anterior and posterior canal regions close to the cell body (arrowheads). (A, D, G) GFP channel, (B) Nomarksi, (C) close-up of the region, where the AVG cell body is located (overlay of Nomarksi and CFP channel, showing *odr-2*::CFP expression in RIF and AVG (arrow) cell bodies. (D–F) colocalization of PLR-1::GFP and *odr-2*::CFP in AVG (arrow). (D, E) single channel, (F) overlay. Scale bar: 10 μm.

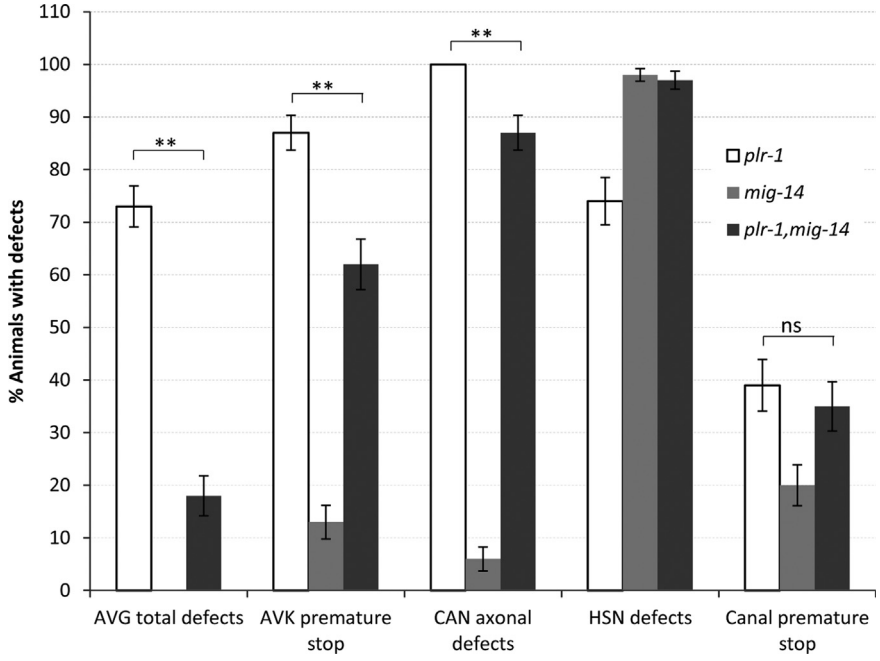

Fig. 6. Suppression of AVG defects by *mig-14*. Columns are percentages of animals with defects (± standard error) with genotypes as indicated. Different types of defects are also indicated. For each strain $n > 100$ except *mig-14*; HSN ($n=51$) and *plr-1*; HSN ($n=98$) animals were analyzed. χ^2 tests were used to determine whether double mutants are significantly different from the strongest single mutant (**$p < 0.01$; ^{ns}: not significant). Mutant alleles used: *plr-1*(*hd129*) and *mig-14*(*ga62*). Fluorescent markers used: AVG marker (*odr-2*::*tdTomato*), AVK marker (*flp-1*::GFP), CAN marker (*ceh-23*:: GFP), HSN marker (*tph-1*:: GFP) and excretory canal marker (*pgp-12*:: GFP).

Discussion

plr-1 affects multiple aspects of neuronal development

We identified alleles of *plr-1* in a forward genetic screen for outgrowth and navigation of the ventral nerve cord pioneer axon. *plr-1* mutant animals show a variety of defects including a polarity reversal of the AVG neuron, premature termination of axonal outgrowth and aberrant midline crossing of the AVG axon. While the polarity reversal defects seem to be limited to AVG, we found outgrowth defects in additional axons as well as in non-neuronal processes such as the excretory canals. A common theme is that

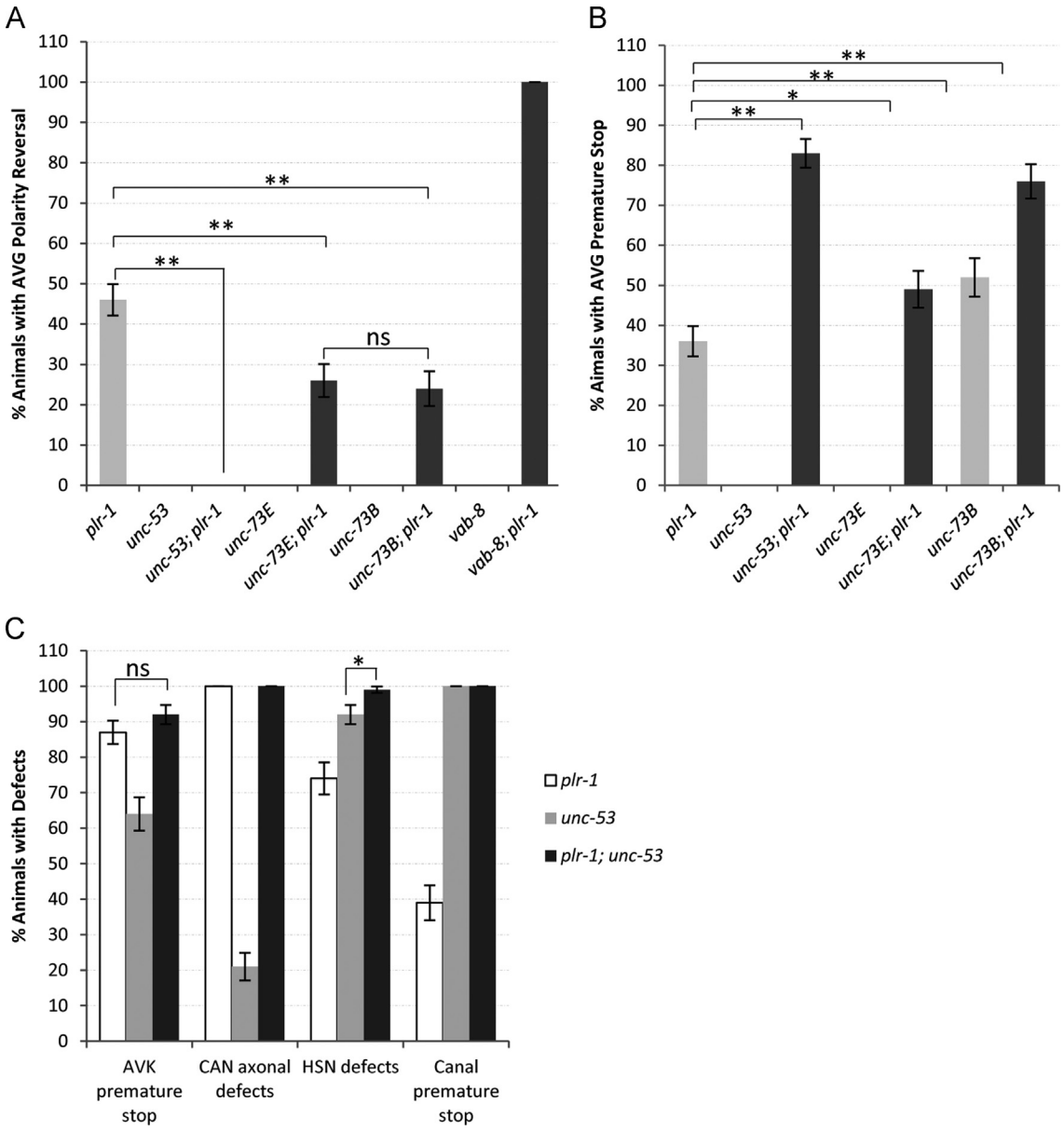

Fig. 7. *plr-1* interacts genetically with *unc-53*, *unc-73* and *vab-8*. Columns represent percentage animals with (A) polarity reversal defects and (B) AVG premature stop defects (± standard error). (C) The percentage of animals with indicated defects (± standard error) in other neuronal and non-neuronal cells. Genotypes are as indicated. For each strain $n \geq 100$ animals were analyzed. χ^2 tests were used to determine whether double mutants are significantly different from the stronger single mutant ($^*p < 0.05$; $^{**}p < 0.01$; ^{ns}: not significant). Mutant alleles used: *plr-1*(*hd129*), *unc-53*(*n116*), *unc-73E*(*ev802*), *unc-73B*(*rh40*) and *vab-8*(*e1017*). Fluorescent markers used: AVG marker (*inx-18*::GFP), AVK marker (*flp-1*::GFP), CAN marker (*ceh-23*::GFP), HSN marker (*tph-1*::GFP) and excretory canal marker (*pgp-12*::GFP).

only posteriorly directed processes are affected and that processes can grow most of the distance and typically stop short at variable positions only in the posterior half of the animal. While individual aspects of the *plr-1* phenotype such as polarity reversals or axonal outgrowth defects are shared with other mutants, the combination of defects seen in *plr-1* mutants is rather unique and not found in other mutants so far.

plr-1 encodes a putative E3 ligase

PLR-1 is predicted to be an E3 ligase. E3 ligases are part of the enzyme complex which transfers ubiquitin to substrate proteins in preparation for degradation by the proteosomal complex (Hershko and Ciechanover, 1982; Hershko et al., 2000). E3 ligases provide substrate specificity by bringing the target protein in contact with the E2 ubiquitin-conjugating enzyme. Ubiquitination by E3 ligases is also used to regulate receptor internalization from the cell surface and protein transport in endocytic compartments of the cell (d'Azzo et al., 2005; Hicke and Dunn, 2003). PLR-1 has a signal peptide and transmembrane domain, which suggests that it enters the secretory pathway. PLR-1 protein has been shown to localize to various endosomal compartments in particular early endosomes (Moffat et al., 2014). PLR-1 promotes endocytosis of Wnt receptors from the cell surface (Moffat et al., 2014). Similarly the vertebrate homologues RNF43 and ZNRF3 also induce the endocytosis of Wnt receptors such as frizzled and LRP6 (Hao et al., 2012; Koo et al., 2012). Both the ectodomain and the RING finger domain of RNF43 are necessary for the binding and internalization of Wnt receptor frizzled FZD5 (Koo et al., 2012). Similarly both the ectodomain and the RING finger domain of PLR-1 are required for this activity (Moffat et al., 2014).

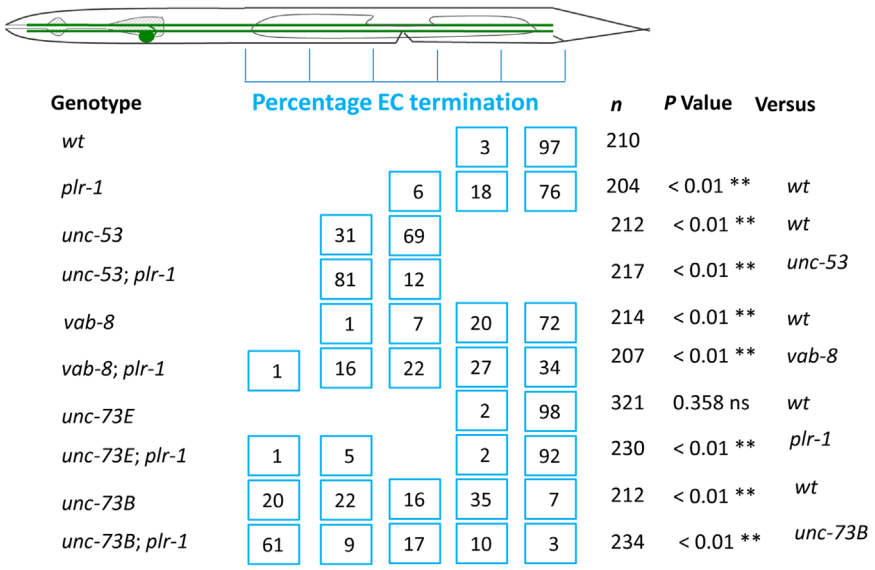

Fig. 8. Genetic analysis of posterior excretory canal defects. For genetic interactions in excretory canals, scoring and analysis was done according to Marcus-Gueret et al. (2012), also described in the *Materials and methods*. Numbers in the boxes represent the percentage of excretory canal termination points in that region. Genotypes and the number of canals analyzed are as indicated (wt is wild type). χ^2 tests were used to determine statistical significance ($^{**}p < 0.01$; ^{ns}: not significant). Alleles used are: *plr-1* (*hd129*), *unc-53*(*n166*), *vab-8*(*e1017*). *unc-73E*(*ev802*) *and unc-73B*(*rh40*). Fluorescent marker used: *pgp-12*::GFP.

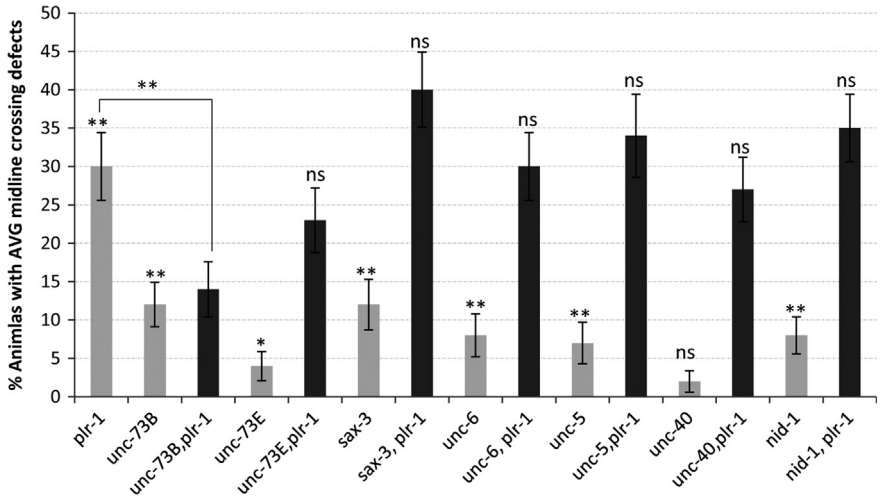

Fig. 9. Genetic analysis of AVG midline crossing defects. For this analysis only those animals were counted in which the AVG axon extended beyond the vulva into the posterior half of the animal indicating normal polarity of AVG. Columns represent the percentage of animals with AVG midline crossing defects (± standard error) with different single mutants (light grey shaded) and *plr-1* double mutants (black shaded). For each strain $n \geq 100$ animals were analyzed. χ^2 tests were used to establish statistical significance between the mutants. Single mutants were compared with wild type and double mutants were compared with *plr-1* single mutant ($^{*}p < 0.05$; $^{**}p < 0.01$; ^{ns}: not significant). Mutant alleles used: *plr-1*(*hd129*), *sax-3*(*ky123*), *unc-73E*(*ev802*), *unc-73B*(*rh40*), *unc-6*(*ev400*), *unc-5*(*e53*), *unc-40*(*e271*) and *nid-1*(*cg119*). Fluorescent marker used: *odr-2*::*tdTomato*.

These data suggest that PLR-1 affects neuronal development indirectly by regulating the availability of Wnt receptors (and potentially other receptors) at the cell surface.

plr-1 and Wnt signalling

The *C. elegans* genome encodes five Wnt genes (Herman et al., 1995; Maloof et al., 1999; Shackleford et al., 1993; Thorpe et al., 1997), which control a variety of developmental processes (Gleason and Eisenmann, 2010; Gleason et al., 2006; Goldstein et al., 2006; Green et al., 2008; Song et al., 2010). Several neuronal cell migrations are influenced by Wnts (Hilliard and Bargmann, 2006; Pan et al., 2006) and Wnts control the polarity of certain neurons, most notably ALM and PLM (Hilliard and Bargmann, 2006; Prasad and Clark, 2006). The ALM neurons have a short posterior neurite and a much longer anterior neurite (White et al., 1986). In animals with mutations in the Wnt genes *cwn-1* and *egl-20*, ALM sends out a long posterior process and a short anterior process, suggesting that its polarity is reversed (Hilliard and Bargmann, 2006). Strong overexpression of the Wnt *egl-20* or Frizzled receptor *lin-17* in ALM neurons causes similar polarity reversals (Hilliard and Bargmann, 2006). We observed polarity reversals of the AVG neuron, but not of ALM or PLM in *plr-1* mutant animals. *plr-1* induced AVG polarity reversal defects have been linked to excessive Wnt-signalling through the excessive presence of Wnt-receptors on the cell surface of AVG in *plr-1* mutants and *plr-1* has been shown to act cell-autonomously in AVG (Moffat et al., 2014). We found that mutations in *mig-14*/*Wntless* a protein required for the secretion of Wnt proteins (Banziger et al., 2006; Yang et al., 2008) effectively suppress AVG polarity reversal defects, confirming that these defects are indeed likely caused by too much Wnt signalling. Overall the phenotypic

spectrum of *plr-1* mutants shows limited overlap with defects related to Wnt signalling. In particular, AVK, CAN and excretory canal outgrowth defects have not been linked to Wnt signalling. These defects are not effectively suppressed by reducing Wnt-signalling, suggesting that *plr-1* has additional roles unrelated to Wnt receptor presentation at the cell surface.

unc-53/NAV-2 and unc-73/Trio interact with plr-1

UNC-53 is a cytoskeletal regulator required for longitudinal migrations of cells and axons in *C. elegans* (Stringham et al., 2002; Stringham and Schmidt, 2009). Its mammalian homologues called navigators (NAV-1, NAV-2 and NAV-3) are also involved in axon guidance (Maes et al., 2002; Merrill et al., 2002). UNC-53/NAV-2 has been shown to bind to ABI-1 (Abelson kinase interactor), a regulator of Arp2/3 which in turn nucleates actin filaments (Schmidt et al., 2009). Actin regulators such as Ena, WAVE complex, cofilin and profilin regulate neurite formation in mammalian neurons (Tahirovic and Bradke, 2009). UNC-73/Trio is a guanine nucleotide exchange factor (GEF) with separate Rac- and Rho-specific GEF domains. The GEF1 domain activates Rac proteins (MIG-2/RhoG and CED-10/Rac) whereas the GEF2 domain activates RHO-1/Rho (Kubiseski et al., 2003; Spencer et al., 2001; Steven et al., 1998; Wu et al., 2002), which in turn regulate the cytoskeleton and thus play role in cell migrations and axon guidance (Dyer et al., 2010; Spencer et al., 2001). In addition these Rho family GTPases are also involved in establishing polarity in *C. elegans* and mammals (Govek et al., 2005; Levy-Strumpf and Culotti, 2007; Quinn et al., 2008). *unc-53* genetically interacts with the RhoGEF form of *unc-73* along with other cytoskeletal components (Marcus-Gueret et al., 2012) to control posterior extension of excretory canals.

We found that *unc-53* mutants completely suppress the AVG polarity defect in *plr-1* mutants and that *unc-73* mutants partially suppress these defects. Alleles specific to both RacGEF and RhoGEF domains of UNC-73/Trio showed similar suppression, supporting the idea that both Rac and Rho specific effectors are involved in regulating AVG polarity. Since the polarity defects appear to be caused by ectopic Wnt signalling due to the presence of Wnt receptors on the surface of AVG, this suggests that *unc-53* and *unc-73* might negatively influence Wnt signalling. However, neither *unc-53* nor *unc-73* has been implicated in Wnt signalling, so it is currently unclear what the connection to Wnt signalling is. UNC-73/Trio together with VAB-8 has recently been shown to increase the cell surface availability of axon guidance receptors UNC-40/DCC and SAX-3/Robo in neurons (Levy-Strumpf and Culotti, 2007; Watari-Goshima et al., 2007). It is possible that UNC-73 promotes Wnt-receptor expression at the cell surface in AVG. A lack of UNC-73 could lead to the reduced receptor presence at the cell surface counteracting effects of a lack of PLR-1, which would lead to the increased receptor presence. If UNC-73 acts together with VAB-8 in this process, one would expect that mutations in *vab-8* also suppress *plr-1*-induced polarity defects. However, contrary to these expectations, we found that AVG polarity defects are enhanced in *vab-8*; *plr-1* double mutants, indicating that the interactions among *plr-1*, *unc-73* and *vab-8* are more complex in this situation.

plr-1 mutant animals show AVG axon navigation defects in the ventral nerve cord. Our genetic analysis indicated that the RacGEF form of *unc-73* suppresses AVG axon navigation defects, whereas the RhoGEF form of *unc-73* does not. This suggests that *plr-1* genetically interacts specifically with the RacGEF form of *unc-73* for the correct navigation of AVG axon. We found that *plr-1* does not act synergistically with *sax-3*/*Robo* (Slit receptor), *unc-6*/*Netrin* (guidance cue), *unc-5* (receptor for unc-6) and *nid-1*/*Nidogen* (basement membrane component) for AVG axon navigation.

plr-1 mutants have excretory canal outgrowth defects similar to *unc-53*, *unc-73* and *vab-8* mutants (Hedgecock et al., 1987; Stringham et al., 2002; Wightman et al., 1996). UNC-53 acts cell-autonomously together with the RhoGEF form of UNC-73 to control canal outgrowth. In a parallel pathway the RacGEF isoform of UNC-73 acts non-cell-autonomously. Our double mutant analysis indicates that *plr-1* does not act in either of these two pathways implicating a third yet unidentified pathway in this process. Our observation that PLR-1 acts in the excretory cell, suggests that PLR-1 like UNC-53 is required within the excretory cell for the posterior extension of canals but acts through a different genetic pathway. Interactions between PLR-1 and UNC-53 appear to be cell-type specific and different in AVG and the excretory cell adding an additional layer of complexity.

In summary, we have identified a putative E3 ligase, PLR-1, required for several aspect of nervous system development including cell polarity, axon extension and axon navigation in a subset of neurons in *C. elegans*. The cell polarity defects in *plr-1* mutants have recently been found to be secondary consequences of ectopic Wnt signalling and PLR-1 has been shown to remove Wnt receptors from the surface of the AVG neuron (Moffat et al., 2014). Our analysis confirmed that AVG-related defects are likely due to ectopic Wnt-signalling, but that additional defects found in *plr-1* mutants are unrelated to Wnt-signalling, suggesting that *plr-1* has Wnt-independent functions as well. Finally our data implicate *unc-53*/*NAV-2* and *unc-73*/*Trio* in regulating cell polarity together with *plr-1*.

Materials and methods

Nematode strains and alleles used

The following strains were used for phenotypic analysis: *hdIs51* [*odr-2::tdTomato*, *rol-6(su1006)*] X; *otIs182*[*inx-18::GFP*]; *hdIs29*[*odr-2::CFP*,*sra-6::DsRed2*] V; *zdIs13*[*tph-1::GFP*] IV; *gmIs18*[*ceh-23::GFP*]; *hdIs54*[*flp-1::GFP*, *sra-6::plum*, *pha-1(+)*]; *sIs10089*[*pgp-12::GFP*,*him-8*]; *rhIs5*[*glr-1::GFP*,*dpy-20(+)*] X; *zdIs5*[*mec-4::GFP*] I; *evIs111*[*rgef-1::GFP*] V; *hdIs22*[*unc-129::CFP*, *unc-47::DsRed2*] V;

The following alleles were used for phenotypic analysis and genetic interaction studies: *plr-1(hd129)* III, *plr-1(hd128)* III, *plr-1(tm2975)* III, *mig-14(ga62)* II, *unc-53(n116)* II, *unc-73E(ev802)* I, *unc-73B(rh40)* I, *vab-8(e1017)* V, *sax-3(ky123)* X, *unc-6(ev400)* X, *unc-5(e53)* IV, *unc-40 (e271)* I and *nid-1(cg119)* V. The strains were cultured and maintained at 20 °C under standard conditions (Brenner, 1974).

Mapping and gene identification

The *plr-1* alleles *hd128* and *hd129* were isolated after EMS mutagenesis of *hdIs51*[*odr-2*::*tdTomato*] animals by the selection of F2 animals with AVG axon outgrowth defects in a non-clonal screen. The *tm2957* deletion allele was provided by the *C. elegans* Gene Knockout Consortium and National Bioresource project. We mapped both the *hd129* and *hd128* alleles to a 337.6 kb on Chromosome III between SNP-15 and pKP3074. Injection of Fosmids (Geneservices, Cambridge UK) into both alleles narrowed down the region to 34 kb region on the right arm of Chromosome III which only contains two genes, *plr-1*(*Y47D3B.11*) and *bed-2*(*Y447D3B.9*). These two genes are in opposite orientation. Fosmid WRM0636cC10 covers both the genes whereas Fosmid WRM0632aD04 covers only *plr-1* and a part of *bed-2*. Fosmids WRM0636cC10 (4.2 ng/μl) and WRM0632aD04 (5.2 ng/μl) along with *unc-122*::GFP (45 ng/μl) as a co-injection marker were injected into *hd129* animals for rescue. Fosmid WRM0636cC10 rescued the AVG defects of *hd129* animals in two out of two lines and WRM0632aD04 rescued the AVG defects of *hd129* animals in three out of three lines, thus identifying *plr-1*(*Y47D3B.11*) as a most likely candidate. Sequencing the *plr-1*/*Y47D3B.11* coding region in *hd129* animals revealed a 159 bp deletion which completely removes exon 2 leading to a frameshift and premature stop codon. Sequencing

of the *plr-1*/*Y47D3B.11* coding region in *hd128* animals revealed a 132 bp in-frame deletion in exon 4. *tm2957* is a 239 bp deletion in the beginning of exon 4, which results in a frameshift and premature stop codon.

Expression constructs

The promoter reporter construct (*plr-1*::*GFP*) was generated by combining a 3906 bp upstream region of *plr-1* with GFP by using a PCR-based fusion method (Hobert, 2002). Transgenic lines were generated by injecting *plr-1*::GFP (25 ng/μl) along with *pha-1(+)* (pBX) (60 ng/μl) as a co-injection marker (Granato et al., 1994) in *pha-1*(*e2123ts*) animals. The translational reporter construct PLR-1::GFP was generated by tagging the C-terminus of PLR-1 with GFP in the Fosmid WRM0636cC10 by recombineering (Tursun et al., 2009). For all constructs, transgenic animals were generated as described (Mello et al., 1991).

To express *plr-1* specifically in the excretory cell, *pgp-12* promoter (Marcus-Gueret et al., 2012) and *plr-1* cDNA were cloned into GFP vector pPD95.75 (Fire vector kit). This construct (15 ng/μl) was injected along with co-injection marker *unc-122*::*GFP* (45 ng/μl) into *plr-1* mutant animals and the animals from three independent transgenic lines were analyzed for excretory canal defects.

Phenotypic analysis of neuronal and non-neuronal defects

Axonal defects were scored with a Zeiss Axiscope (40x objective) in adult animals expressing fluorescent markers in respective neurons. Animals were immobilized with 10 mM sodium azide in M9 buffer for 1 h and mounted on 3% agar pads before analysis. For excretory canal defects, adult animals expressing the *pgp-12*::GFP reporter were immobilized in the same way. Scoring and analysis of excretory canal defects were done according to Marcus-Gueret et al. (2012).

Microscopy

Confocal images of mixed stage population of animals with respective fluorescent proteins were acquired on a Zeiss Axioplan II microscope (Carl-Zeiss AG, Germany) connected to a Quorum WaveFX spinning disc system (Quorum Technologies, Canada). Stacks of confocal images with 0.2–0.5 μm distance between focal planes were recorded. Image acquisition and analysis were carried out by using Volocity software (Perkin-Elmer, Waltham, MA). Images in the figures are maximum intensity projections of all focal planes. Figures and GFP/Nomarski overlays were assembled with Adobe photoshop CS8.0 (Adobe, San Jose, CA, USA).

Genetic interactions

To test genetic interactions between *plr-1* and potential interacting genes, phenotypes of both single and double mutants were examined. Two genes are thought to act in the same pathway if the penetrance of double mutant phenotype is similar to that of the strongest single mutant. χ^2 tests were used to determine statistical significance between double mutants and the strongest single mutant. For excretory canals, scoring and analysis were done according to Marcus-Gueret et al. (2012). The posterior part of the body was divided into five regions (1–5) from the turning point of the anterior gonad arm to the tail as shown in Fig. 8. The termination point of the canal was determined under the microscope using a GFP marker expressed in the canal. Phenotypes were grouped into two categories—wild type (scored as 5) and premature canal termination (scored as <5). Single mutants were compared with the wild type and double mutants were compared with the strongest single mutants, which was set as baseline for comparison while phenotypes showing further reduction in canal extensions were grouped together.

Acknowledgements

We would like to thank members of the Hutter lab for comments on the manuscript and the Stringham, Hawkins and Buechner labs for strains. Some of the nematode strains used in this work were provided by the *Caenorhabditis* Genetics Center, which is funded by NIH Office of Research Infrastructure Programs (P40 OD010440). One *plr-1* allele was provided by the *C. elegans* National Bioresource Project (Japan). This work was supported by NSERC (Grant 312498-2012) and CIHR (Grant MOP 93719).

References

Banziger, C., Soldini, D., Schutt, C., Zipperlen, P., Hausmann, G., Basler, K., 2006. Wntless, a conserved membrane protein dedicated to the secretion of Wnt proteins from signaling cells. Cell 125, 509–522.
Brenner, S., 1974. The genetics of *Caenorhabditis elegans*. Genetics 77, 71–94.
Chitnis, A.B., Kuwada, J.Y., 1991. Elimination of a brain tract increases errors in path finding by follower growth cones in the zebrafish embryo. Neuron 7, 277–285.
Colavita, A., Krishna, S., Zheng, H., Padgett, R.W., Culotti, J.G., 1998. Pioneer axon guidance by UNC-129, a *C. elegans* TGF-beta. Science 281, 706–709.
d'Azzo, A., Bongiovanni, A., Nastasi, T., 2005. E3 ubiquitin ligases as regulators of membrane protein trafficking and degradation. Traffic 6, 429–441.
Durbin, R.M., 1987. Studies on the Development and Organisation of the Nervous System of *Caenorhabditis elegans*. Ph.D. dissertation, University of Cambridge, England.
Dyer, J.O., Demarco, R.S., Lundquist, E.A., 2010. Distinct roles of Rac GTPases and the UNC-73/Trio and PIX-1 Rac GTP exchange factors in neuroblast protrusion and migration in *C. elegans*. Small GTPases 1, 44–61.
Eisenmann, D.M., Kim, S.K., 2000. Protruding vulva mutants identify novel loci and Wnt signaling factors that function during *Caenorhabditis elegans* vulva development. Genetics 156, 1097–1116.
Gleason, J.E., Eisenmann, D.M., 2010. Wnt signaling controls the stem cell-like asymmetric division of the epithelial seam cells during *C. elegans* larval development. Dev. Biol. 348, 58–66.
Gleason, J.E., Szyleyko, E.A., Eisenmann, D.M., 2006. Multiple redundant Wnt signaling components function in two processes during *C. elegans* vulval development. Dev. Biol. 298, 442–457.
Goldstein, B., Takeshita, H., Mizumoto, K., Sawa, H., 2006. Wnt signals can function as positional cues in establishing cell polarity. Dev. Cell 10, 391–396.
Goodman, C.S., 1996. Mechanisms and molecules that control growth cone guidance. Annu. Rev. Neurosci. 19, 341–377.
Govek, E.E., Newey, S.E., Van Aelst, L., 2005. The role of the Rho GTPases in neuronal development. Genes Dev. 19, 1–49.
Granato, M., Schnabel, H., Schnabel, R., 1994. pha-1, a selectable marker for gene transfer in *C. elegans*. Nucleic Acids Res. 22, 1762–1763.
Green, J.L., Inoue, T., Sternberg, P.W., 2008. Opposing Wnt pathways orient cell polarity during organogenesis. Cell 134, 646–656.
Hao, H.X., Xie, Y., Zhang, Y., Charlat, O., Oster, E., Avello, M., Lei, H., Mickanin, C., Liu, D., Ruffner, H., Mao, X., Ma, Q., Zamponi, R., Bouwmeester, T., Finan, P.M., Kirschner, M.W., Porter, J.A., Serluca, F.C., Cong, F., 2012. ZNRF3 promotes Wnt receptor turnover in an R-spondin-sensitive manner. Nature 485, 195–200.
Hao, J.C., Yu, T.W., Fujisawa, K., Culotti, J.G., Gengyo-Ando, K., Mitani, S., Moulder, G., Barstead, R., Tessier-Lavigne, M., Bargmann, C.I., 2001. *C. elegans* slit acts in midline, dorsal–ventral, and anterior–posterior guidance via the SAX-3/Robo receptor. Neuron 32, 25–38.
Harris, J., Honigberg, L., Robinson, N., Kenyon, C., 1996. Neuronal cell migration in *C. elegans*: regulation of Hox gene expression and cell position. Development 122, 3117–3131.
Hedgecock, E.M., Culotti, J.G., Hall, D.H., 1990. The unc-5, unc-6, and unc-40 genes guide circumferential migrations of pioneer axons and mesodermal cells on the epidermis in *C. elegans*. Neuron 4, 61–85.
Hedgecock, E.M., Culotti, J.G., Hall, D.H., Stern, B.D., 1987. Genetics of cell and axon migrations in *Caenorhabditis elegans*. Development 100, 365–382.
Herman, M.A., Vassilieva, L.L., Horvitz, H.R., Shaw, J.E., Herman, R.K., 1995. The *C. elegans* gene lin-44, which controls the polarity of certain asymmetric cell divisions, encodes a Wnt protein and acts cell nonautonomously. Cell 83, 101–110.
Hershko, A., Ciechanover, A., 1982. Mechanisms of intracellular protein breakdown. Annu. Rev. Biochem. 51, 335–364.
Hershko, A., Ciechanover, A., Varshavsky, A., 2000. Basic medical research award. The ubiquitin system. Nat. Med. 6, 1073–1081.
Hicke, L., Dunn, R., 2003. Regulation of membrane protein transport by ubiquitin and ubiquitin-binding proteins. Annu. Rev. Cell Dev. Biol. 19, 141–172.
Hidalgo, A., Brand, A.H., 1997. Targeted neuronal ablation: the role of pioneer neurons in guidance and fasciculation in the CNS of Drosophila. Development 124, 3253–3262.

Hilliard, M.A., Bargmann, C.I., 2006. Wnt signals and frizzled activity orient anterior–posterior axon outgrowth in *C. elegans*. Dev. Cell 10, 379–390.
Hobert, O., 2002. PCR fusion-based approach to create reporter gene constructs for expression analysis in transgenic *C. elegans*. Biotechniques 32, 728–730.
Hutter, H., 2003. Extracellular cues and pioneers act together to guide axons in the ventral cord of *C. elegans*. Development 130, 5307–5318.
Ishii, N., Wadsworth, W.G., Stern, B.D., Culotti, J.G., Hedgecock, E.M., 1992. UNC-6, a laminin-related protein, guides cell and pioneer axon migrations in *C. elegans*. Neuron 9, 873–881.
Keynes, R., Cook, G.M., 1995. Axon guidance molecules. Cell 83, 161–169.
Klose, M., Bentley, D., 1989. Transient pioneer neurons are essential for formation of an embryonic peripheral nerve. Science 245, 982–984.
Koo, B.K., Spit, M., Jordens, I., Low, T.Y., Stange, D.E., van de Wetering, M., van Es, J.H., Mohammed, S., Heck, A.J., Maurice, M.M., Clevers, H., 2012. Tumour suppressor RNF43 is a stem-cell E3 ligase that induces endocytosis of Wnt receptors. Nature 488, 665–669.
Kubiseski, T.J., Culotti, J., Pawson, T., 2003. Functional analysis of the *Caenorhabditis elegans* UNC-73B PH domain demonstrates a role in activation of the Rac GTPase in vitro and axon guidance in vivo. Mol. Cell. Biol. 23, 6823–6835.
Levy-Strumpf, N., Culotti, J.G., 2007. VAB-8, UNC-73 and MIG-2 regulate axon polarity and cell migration functions of UNC-40 in *C. elegans*. Nat. Neurosci. 10, 161–168.
Maes, T., Barcelo, A., Buesa, C., 2002. Neuron navigator: a human gene family with homology to unc-53, a cell guidance gene from *Caenorhabditis elegans*. Genomics 80, 21–30.
Maloof, J.N., Whangbo, J., Harris, J.M., Jongeward, G.D., Kenyon, C., 1999. A Wnt signaling pathway controls hox gene expression and neuroblast migration in *C. elegans*. Development 126, 37–49.
Marcus-Gueret, N., Schmidt, K.L., Stringham, E.G., 2012. Distinct cell guidance pathways controlled by the Rac and Rho GEF domains of UNC-73/TRIO in *Caenorhabditis elegans*. Genetics 190, 129–142.
McConnell, S.K., Ghosh, A., Shatz, C.J., 1989. Subplate neurons pioneer the first axon pathway from the cerebral cortex. Science 245, 978–982.
Mello, C.C., Kramer, J.M., Stinchcomb, D., Ambros, V., 1991. Efficient gene transfer in *C. elegans*: extrachromosomal maintenance and integration of transforming sequences. EMBO J. 10, 3959–3970.
Merrill, R.A., Plum, L.A., Kaiser, M.E., Clagett-Dame, M., 2002. A mammalian homolog of unc-53 is regulated by all-trans retinoic acid in neuroblastoma cells and embryos. Proc. Natl. Acad. Sci. USA 99, 3422–3427.
Moffat, L.L., Robinson, R.E., Bakoulis, A., Clark, S.G., 2014. The conserved transmembrane RING finger protein PLR-1 downregulates Wnt signaling by reducing Frizzled, Ror and Ryk cell-surface levels in *C. elegans*. Development 141, 617–628.
Pan, C.L., Howell, J.E., Clark, S.G., Hilliard, M., Cordes, S., Bargmann, C.I., Garriga, G., 2006. Multiple Wnts and frizzled receptors regulate anteriorly directed cell and growth cone migrations in *Caenorhabditis elegans*. Dev. Cell 10, 367–377.
Prasad, B.C., Clark, S.G., 2006. Wnt signaling establishes anteroposterior neuronal polarity and requires retromer in *C. elegans*. Development 133, 1757–1766.
Quinn, C.C., Pfeil, D.S., Wadsworth, W.G., 2008. CED-10/Rac1 mediates axon guidance by regulating the asymmetric distribution of MIG-10/lamellipodin. Curr. Biol. 18, 808–813.
Schmidt, K.L., Marcus-Gueret, N., Adeleye, A., Webber, J., Baillie, D., Stringham, E.G., 2009. The cell migration molecule UNC-53/NAV2 is linked to the ARP2/3 complex by ABI-1. Development 136, 563–574.
Shackleford, G.M., Shivakumar, S., Shiue, L., Mason, J., Kenyon, C., Varmus, H.E., 1993. Two wnt genes in *Caenorhabditis elegans*. Oncogene 8, 1857–1864.
Song, S., Zhang, B., Sun, H., Li, X., Xiang, Y., Liu, Z., Huang, X., Ding, M., 2010. A Wnt-Frz/Ror-Dsh pathway regulates neurite outgrowth in *Caenorhabditis elegans*. PLoS Genet. 6 (8), e1001056.
Spencer, A.G., Orita, S., Malone, C.J., Han, M., 2001. A RHO GTPase-mediated pathway is required during P cell migration in *Caenorhabditis elegans*. Proc. Natl. Acad. Sci. USA 98, 13132–13137.
Steven, R., Kubiseski, T.J., Zheng, H., Kulkarni, S., Mancillas, J., Ruiz Morales, A., Hogue, C.W., Pawson, T., Culotti, J., 1998. UNC-73 activates the Rac GTPase and is required for cell and growth cone migrations in *C. elegans*. Cell 92, 785–795.
Stringham, E., Pujol, N., Vandekerckhove, J., Bogaert, T., 2002. unc-53 controls longitudinal migration in *C. elegans*. Development 129, 3367–3379.
Stringham, E.G., Schmidt, K.L., 2009. Navigating the cell: UNC-53 and the navigators, a family of cytoskeletal regulators with multiple roles in cell migration, outgrowth and trafficking. Cell Adhes. Migr. 3, 342–346.
Tahirovic, S., Bradke, F., 2009. Neuronal polarity. Cold Spring Harb. Perspect. Biol. 1, a001644.
Tessier-Lavigne, M., Goodman, C.S., 1996. The molecular biology of axon guidance. Science 274, 1123–1133.
Thorpe, C.J., Schlesinger, A., Carter, J.C., Bowerman, B., 1997. Wnt signaling polarizes an early *C. elegans* blastomere to distinguish endoderm from mesoderm. Cell 90, 695–705.
Tursun, B., Cochella, L., Carrera, I., Hobert, O., 2009. A toolkit and robust pipeline for the generation of fosmid-based reporter genes in *C. elegans*. PLoS One 4, e4625.
Watari-Goshima, N., Ogura, K., Wolf, F.W., Goshima, Y., Garriga, G., 2007. *C. elegans* VAB-8 and UNC-73 regulate the SAX-3 receptor to direct cell and growth-cone migrations. Nat. Neurosci. 10, 169–176.
White, J., Southgate, E., Thomson, J., Brenner, S., 1986. The structure of the nervous system of the nematode *Caenorhabditis elegans*. Philos. Trans. R. Soc. Lond. B 314, 1–340.
Wightman, B., Clark, S.G., Taskar, A.M., Forrester, W.C., Maricq, A.V., Bargmann, C.I., Garriga, G., 1996. The *C. elegans* gene vab-8 guides posteriorly directed axon outgrowth and cell migration. Development 122, 671–682.
Wolf, F.W., Hung, M.S., Wightman, B., Way, J., Garriga, G., 1998. vab-8 is a key regulator of posteriorly directed migrations in *C. elegans* and encodes a novel protein with kinesin motor similarity. Neuron 20, 655–666.
Wu, Y.C., Cheng, T.W., Lee, M.C., Weng, N.Y., 2002. Distinct rac activation pathways control *Caenorhabditis elegans* cell migration and axon outgrowth. Dev. Biol. 250, 145–155.
Yamamoto, Y., Takeshita, H., Sawa, H., 2011. Multiple Wnts redundantly control polarity orientation in *Caenorhabditis elegans* epithelial stem cells. PLoS Genet. 7, e1002308.
Yang, P.T., Lorenowicz, M.J., Silhankova, M., Coudreuse, D.Y., Betist, M.C., Korswagen, H.C., 2008. Wnt signaling requires retromer-dependent recycling of MIG-14/Wntless in Wnt-producing cells. Dev. Cell 14, 140–147.